

A Well-Defined Pd Hybrid Material for the Z-Selective Semihydrogenation of Alkynes Characterized at the Molecular Level by DNP SENS**

Matthew P. Conley,^[a] Ruben M. Drost,^[b] Mathieu Baffert,^[c] David Gajan,^[a] Cornelis Elsevier,^[b] W. Trent Franks,^[d] Hartmut Oschkinat,^[d] Laurent Veyre,^[c] Alexandre Zagdoun,^[e] Aaron Rossini,^[e] Moreno Lelli,^[e] Anne Lesage,^[e] Gilles Casano,^[f] Olivier Ouari,^[f] Paul Tordo,^[f] Lyndon Emsley,^{*[e]} Christophe Copéret,^{*[a]} and Chloé Thieuleux^{*[c]}

The detailed characterization of catalytic materials lays the foundation for quantitative structure–activity relationships that lead to rational design of catalysts. However, most classical solid catalysts are difficult to characterize at the molecular level, even when using the most advanced analytical techniques available to surface science. Thus, the vast majority of chemical reactions that are performed with heterogeneous catalysts lack characterized molecular structures. In contrast, homogeneous catalysts contain single metal sites in well-defined ligand environments, structures of which can be readily solved by spectroscopic or diffraction methods. The knowledge of structure gives fundamental insight into the behavior of a homogeneous complex under catalytic

conditions, which then directly leads to improved catalyst design. Construction of materials that contain metal complexes supported on a material surface and having controlled first-coordination-sphere environments bridges this gap between homogeneous and heterogeneous catalysis,^[1] giving catalysts that are readily separable from the reaction medium and that avoid metal contamination of the end product.

However, one of the critical barriers to overcome in the production of these molecularly defined materials is the determination of the structure of the surface sites. Though NMR spectroscopy is a powerful method to determine the structure of such solids,^[2] the low inherent sensitivity of NMR spectroscopy coupled with the small quantity of catalytic sites in these materials renders conventional NMR characterization extremely difficult. Recently, we have shown in model systems how dynamic nuclear polarization (DNP) could be used to selectively amplify the NMR signal from surface species, leading to remarkable signal enhancements (up to 100) and to large reduction in experimental times.^[3] Herein, we describe the first application of this approach to the characterization of a well-defined catalytic system, namely, a hybrid material containing uniformly distributed Pd–N heterocyclic carbenes (NHC) complexes within the mesoporous network of a silica matrix. We show that by using an appropriate solvent/radical system for impregnation and by taking care that the surface is correctly passivated, the DNP–surface-enhanced NMR spectroscopy (SENS) method leads to the full structural determination of the Pd surface complexes, in a manner analogous to what would be done for homogeneous catalysts with solution NMR. We then show that, as was expected from its well-defined structure and environment, this material is an efficient precatalyst for the Z-selective semihydrogenation of alkynes.

The catalytic reduction of alkynes to Z-olefins (Eq. [1]) is classically performed with the Lindlar catalyst,^[4] a heterogeneous catalyst that consists of palladium particles supported on CaCO_3 doped with lead acetate. Quinoline is also added to this mixture to poison most of the surface palladium sites, preventing over-reduction of Z-ene products. Though recent

[a] Dr. M. P. Conley, Dr. D. Gajan, Prof. Dr. C. Copéret
Laboratory of Inorganic Chemistry, ETH Zürich
Wolfgang Pauli Strasse 10, 8093 Zürich (Switzerland)
E-mail: ccoperet@inorg.chem.ethz.ch

[b] R. M. Drost, Prof. Dr. C. Elsevier
Van't Hoff Institute for Molecular Sciences
University of Amsterdam
Science Park 904, 1098XH Amsterdam (The Netherlands)

[c] Dr. M. Baffert, L. Veyre, Dr. C. Thieuleux
Université Lyon, Institut de Chimie de Lyon
UMR C2P2 CNRS-UCBL-ESCPELyon
Equipe Chimie Organométallique de Surface
43 Bd. du 11 Novembre 1918, 69616 Villeurbanne (France)
E-mail: thieuleux@cpe.fr

[d] Dr. W. T. Franks, Prof. Dr. H. Oschkinat
NMR Supported Structural Biology
Leibniz-Institute für Molekulare Pharmakologie (FMP)
Robert-Roessle-Strasse 10, 13125 Berlin (Germany)

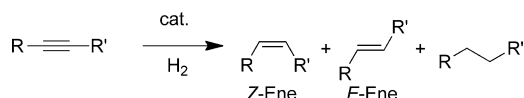
[e] A. Zagdoun, Dr. A. Rossini, Dr. M. Lelli, Dr. A. Lesage,
Prof. Dr. L. Emsley
Centre de RMN à Très Hauts Champs
Institut des Sciences Analytiques
Université de Lyon (CNRS/ENS Lyon/UCB Lyon 1)
5, rue de la Doua, 69100 Villeurbanne (France)
E-mail: lyndon.emsley@ens-lyon.fr

[f] Dr. G. Casano, Dr. O. Ouari, Prof. Dr. P. Tordo
Aix-Marseille Université, CNRS, ICR UMR 7273
Faculté de Saint Jérôme case 521, 13397 Marseille cedex 20 (France)

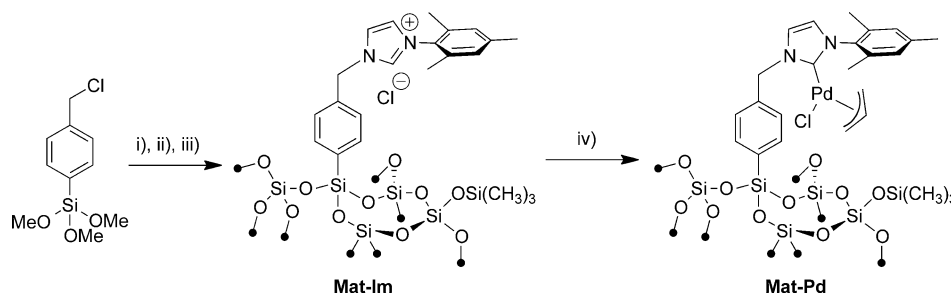
[**] DNP SENS=Dynamic nuclear polarization surface-enhanced spectroscopy.

 Supporting information for this article is available on the WWW under <http://dx.doi.org/10.1002/chem.201302484>.

progress has shown that Pd particles^[5] and even gold surfaces^[6] can catalyze the selective semihydrogenation of alkynes,^[7] the catalytically active site in Lindlar's catalyst remains unknown,^[8] and optimizing this system often relies on empirical observations as opposed to quantitative structure activity relationships.



In selective alkyne semihydrogenation, homogeneous Pd complexes that contain bis(arylimino)acenaphthene (Arbian) or NHC ligands have also been developed to selectively give *Z*-alkenes.^[9] Herein, we have prepared the corresponding immobilized system that contains palladium–NHC complexes incorporated into a mesostructured silica material (Mat-Pd) by reaction of $[\pi\text{-C}_3\text{H}_5\text{PdCl}]_2$ with the imidazolium functionalities distributed in the pore channels of a mesoporous hybrid material (Scheme 1).^[10] The material containing imidazolium units (Mat-Im) was prepared by 1) the



Scheme 1. Synthesis of Mat-Pd: i) TEOS (28 equiv), HCl/H₂O (pH 1.5), P123, NaF, 45 °C, 4 days; ii) mesitylimidazole (10 equiv), toluene, reflux, 16 h; iii) TMSCl, Et₃N, toluene, 25 °C, 16 h; iv) KHMDS (1 equiv), THF followed by $[\pi\text{-C}_3\text{H}_5\text{PdCl}]_2$ (2 equiv Pd).

co-hydrolysis and co-condensation of Si(OEt)₄ and (*para*-chlorophenylmethyl)trimethoxysilane in the presence of Pluronic 123, a structure-directing agent;^[11] 2) the subsequent treatment of this material with mesitylimidazole; and 3) the passivation of the surface silanols with (CH₃)₃SiCl/Et₃N to give Mat-Im. We also prepared the corresponding materials, in which the surface was passivated with (CD₃)₃SiCl/Et₃N in place of (CH₃)₃SiCl/Et₃N to give [D₉]Mat-Im, because we have observed that trimethylsilyl (TMS)-passivated materials, which are essential for metal-complex incorporation, obfuscate the DNP NMR signal enhancements necessary for the characterization discussed below, due to the high density of fast-relaxing methyl protons.^[12] Deuteration of the surface methyl groups restores the DNP performance. Treatment of Mat-Im and [D₉]Mat-Im with potassium hexamethyldisilazide (KHMDS) in THF suspension and subsequent addition of $[\pi\text{-C}_3\text{H}_5\text{PdCl}]_2$ gave Mat-Pd and [D₉]Mat-Pd, respectively (Scheme 1, Figure 1a).

The ligand precursor (Mat-Im) and the Pd–NHC catalyst (Mat-Pd) were fully characterized by DNP SENS analysis.^[3,13] Spectra were recorded on a commercial Bruker 400 MHz/263 GHz gyrotron DNP system (9.4 T) by using samples impregnated with a 16 mm solution of bis(cyclohexyl-TEMPO-bisketal (bCTbK; TEMPO=2,2,6,6-tetramethylpiperidin-1-yl)oxyl) in 1,1,2,2-tetrachloroethane (C₂H₂Cl₄).^[14] Microwave irradiation of the NMR sample at 100 K saturates the EPR transitions of bCTbK, and subsequent transfer of polarization from the electrons to the nuclei of interest on the surface resulted in large NMR signal enhancements. Figure 1b shows the ¹³C CPMAS spectra of [D₉]Mat-Im (top spectrum) and [D₉]Mat-Pd (bottom spectrum) at natural isotopic abundance. Surface signal enhancement factors $\varepsilon_{^{13}\text{C},\text{CP}}$ (defined as the ratio of integrated intensities in spectra acquired with and without microwave irradiation) of 25 and 15 were obtained for the aromatic carbons of [D₉]Mat-Im and [D₉]Mat-Pd, respectively. These signal amplification factors (illustrated in Figure 1b for the ligand precursor) translate into a spectacular reduction in experimental time (up to a factor of 625 with respect to standard NMR instrumentation) and allowed the complete structural characterization of both materials by using multidimensional NMR methods. For a comparison, the ¹³C CPMAS spectrum of Mat-Pd is included in the Supporting Information, the signal-to-noise ratio of this spectrum is lower for the surface nuclei after 24 h of acquisition than the SENS spectrum of [D₉]Mat-Pd after 35 min (Figure S11 in the Supporting Information). Clearly, the multi-dimensional data presented below would not be possible without SENS technology.

The ¹³C CPMAS spectrum of [D₉]Mat-Im was fully assigned from a 2D ¹H–¹³C heteronuclear correlation (HETCOR) spectrum (Figure S9 in the Supporting Information). The complete ¹H, ¹³C, and ²⁹Si chemical-shift values are reported in Table S2 in the Supporting Information.

Clear changes were observed in the ¹³C CPMAS spectrum upon the conversion of [D₉]Mat-Im to [D₉]Mat-Pd (Figure 1c). The ¹³C NMR spectrum contains a new signal at $\delta = 109$ ppm together with a significant increase in the resonance intensity of the peaks at 0 and 54 ppm relative to [D₉]Mat-Im. The new resonances at $\delta = 54$ and 110 ppm correspond to two of the expected signals from the Pd–allyl fragment (carbons 9' and 10'). The peak at $\delta = 0$ ppm is assigned to the carbons of the surface OSi(CD₃)₃ groups, and to the methyl carbons of a residual amount of unreacted KHMDS used in the synthesis of [D₉]Mat-Pd. By using a longer cross-polarization contact time of 6 ms, the NHC–Pd carbon resonance is observed at $\delta = 181$ ppm, which consti-

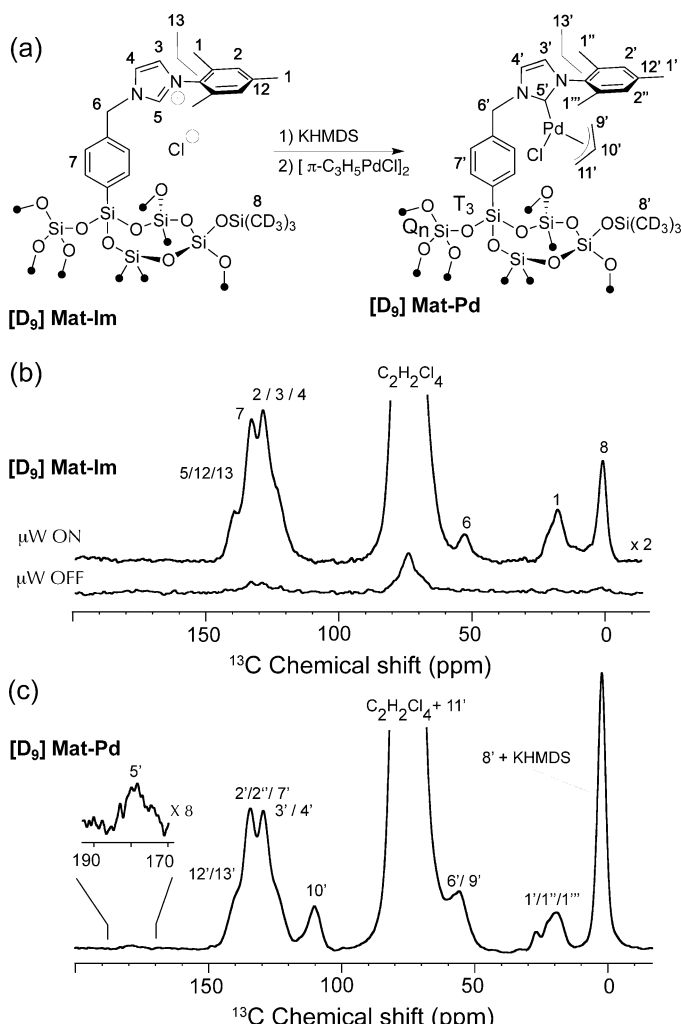


Figure 1. a) Structures of $[D_9]Mat\text{-Im}$ and $[D_9]Mat\text{-Pd}$. b) 1^{H} - ^{13}C HETCOR NMR spectra recorded on $[D_9]Mat\text{-Im}$. c) 1^{H} - ^{13}C HETCOR NMR spectra recorded on $[D_9]Mat\text{-Pd}$.

tutes clear evidence for the attachment of the Pd-allyl fragment to the surface-bound NHC. Previous work on similar metal-containing hybrid materials required tedious and expensive ^{13}C isotopic-labeling strategies to observe this key resonance.

The assignment of the ^{13}C CPMAS spectrum of $[D_9]Mat\text{-Pd}$ was confirmed by a series of ^1H - ^{13}C 2D HETCOR NMR experiments recorded with various CP contact times (250 μs , 2, and 6 ms). The short contact time primarily allows the detection of correlations between bonded pairs of nuclei (Figure 2 a). The correlation at $[\delta_{\text{H}}, \delta_{\text{C}}] = [5.0, 110 \text{ ppm}]$ corresponds to the central Pd-allyl carbon (C10'). The broad shoulder centered at around $[\delta_{\text{H}}, \delta_{\text{C}}] = [5.5, 54 \text{ ppm}]$ corresponds to both the correlations involving the CH_2N (C6') and the terminal Pd-allyl (C9') carbons. The third Pd-allyl resonance (expected at ca. $[\delta_{\text{H}}, \delta_{\text{C}}] = [4, 72 \text{ ppm}]$ by comparison with molecular complexes) likely resides under the NMR solvent signal ($\text{C}_2\text{H}_2\text{Cl}_4$).

The cross-peak at $[\delta_{\text{H}}, \delta_{\text{C}}] = [7, 133 \text{ ppm}]$ in the 2D HETCOR NMR spectrum corresponds to the aromatic carbons

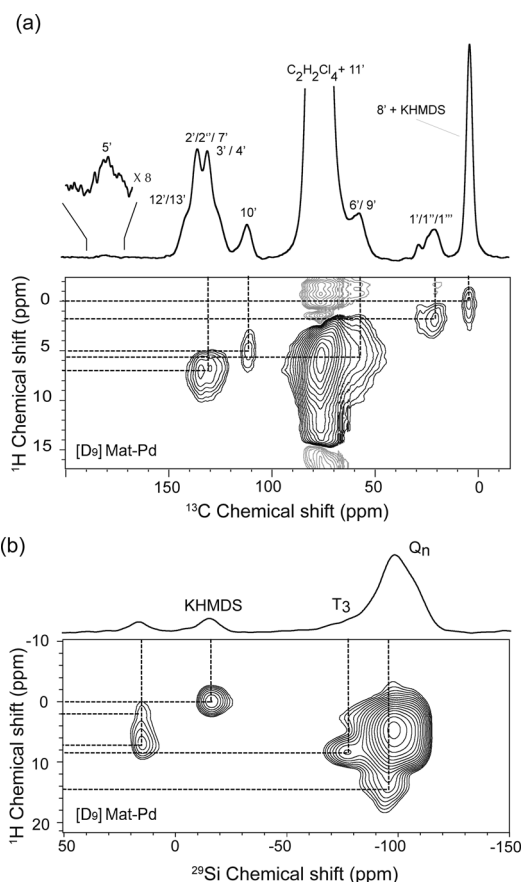


Figure 2. a) Contour plot of a 2D ^1H - ^{13}C HETCOR spectrum recorded on $[D_9]Mat\text{-Pd}$. b) Contour plot of a 2D ^1H - ^{29}Si spectrum recorded on $[D_9]Mat\text{-Pd}$.

of the surface tether (C7') and the mesityl ligand (in particular C2 and C2'), as well as the carbons of the NHC ligand (C3' and C4'). The cross-peak at $[\delta_{\text{H}}, \delta_{\text{C}}] = [2.0, 17 \text{ ppm}]$ is assigned to the methyl groups (C1', C1'' and C1''') of the mesityl function. Finally, the correlation at $[\delta_{\text{H}}, \delta_{\text{C}}] = [0, 0 \text{ ppm}]$ corresponds to surface TMS groups.

At longer contact times, ^1H - ^{13}C HETCOR spectra (Figure S10 in the Supporting Information) display correlations between the terminal Pd-allyl protons (at around 3 ppm) and the central Pd-allyl carbon (C10') at 110 ppm, as was expected. Long-range correlations are also observed at $[\delta_{\text{H}}, \delta_{\text{C}}] = [3.0, 0 \text{ ppm}]$ between these terminal Pd-allyl protons and the carbons of surface trimethylsilyl groups. Similar cross-peaks are visible between the mesityl-methyl protons and carbons of trimethylsilyl moieties at $[\delta_{\text{H}}, \delta_{\text{C}}] = [2.2, 0 \text{ ppm}]$. These correlations reflect spatial proximities between the allyl and mesityl groups on the one hand and the TMS surface groups on the other hand, and suggest that the ligand is bent, interacting with the surface, and that the Pd metal center, therefore, lies close to the silica surface.^[13d, 15] Finally, we note that the Pd-NHC carbene resonance has weak correlations with aromatic and the C10'-Pd-allyl protons, which is also consistent with the structure of the catalyst.

Figure 2b shows a ^1H – ^{29}Si 2D HETCOR NMR spectrum recorded on the $[\text{D}_9]\text{Mat-Pd}$ material. The 1D ^{29}Si NMR spectrum (on top of the 2D plot) contains four resonances corresponding to bulk silicon *Q* sites at $\delta = -98$ ppm, the silicon *T* sites at -77 ppm, the residual unreacted KHMDS signal at -15 ppm, and surface passivating $[\text{D}_9]\text{TMS}$ groups at $\delta = 16$ ppm. The ^1H – ^{29}Si 2D HETCOR spectrum contains the expected correlation between the ^{29}Si *T* site and aromatic proton resonances at around 8 ppm. The $[\text{D}_9]\text{TMS}$ groups show long-range cross-peaks with aromatic protons at $\delta = 7.3$ ppm, as well as correlations with the mesityl methyl groups at 2.0 ppm. The ^{29}Si nuclei of KHMDS at $\delta = -15$ ppm correlate only with their covalently bound methyl protons at 0 ppm. No long-range correlations with other protons were observed, establishing that the KHMDS groups adsorbed onto the surface are well isolated from the rest of the organic residues.

Only two days of measurement time were required to acquire this complete set of experiments (including multiple ^{13}C CP magic-angle spinning (MAS), ^1H – ^{13}C HETCOR, ^{29}Si CP MAS, ^1H – ^{29}Si HETCOR NMR experiments) for the unambiguous assignment of each ^1H , ^{13}C , and ^{29}Si NMR spectrum, and for the full structural characterization of the organometallic fragment. Note that high-resolution MAS (HRMAS) NMR experiments fail on these types of materials. For example, HRMAS on Mat-Im only gave broad spectral lines with poor signal-to-noise ratio in the ^1H and ^{13}C NMR spectra, probably because of the low mobility of surface species, which resulted in strong residual dipolar coupling (see the Supporting Information for details). The NMR data clearly show that the NHC–Pd fragment is in a well-defined molecular environment on the silica surface, that there are no significant side products to the reaction or unreacted ligands, and that the 3D conformation of the surface-bound complex is bent over close to the surface. Such atomic level of characterization was not accessible previously by using any other technique, and would be inconceivable at natural-isotopic abundance without DNP SENS NMR technology.

The catalytic performance of Mat-Pd was evaluated in the stereoselective semihydrogenation of alkynes to *Z*-alkenes in the presence of dihydrogen (Table 1).^[9a,c] The hydrogenation of alkynes (Yne) can give three products: the desired *Z*-alkene (*Z*-Ene), the unwanted *E*-alkene isomer (*E*-Ene), or the over-reduced alkane product (Ane). Mat-Pd is active in semihydrogenation of 1-phenylpropyne (Yne-1) with a turnover frequency (TOF) of 1800 h^{-1} , and kinetically selective towards *Z*-Ene-1 (93%, entry 1). The catalyst is fairly stable under these conditions, allowing a turnover number (TON) of 1100 to be reached for this substrate. However, increasing the substrate to Pd ratio beyond this limit did not lead to full alkyne conversion indicating catalyst deactivation. ICP analysis of the reaction mixtures contains less than 1 ppm palladium, indicating that leaching from the silica support does not occur during catalysis, preventing metal contamination of the final product. This is particularly important, because removing Pd traces from the organic prod-

Table 1. Mat-Pd-catalyzed alkyne semihydrogenation.

Entry	Alkyne	TOF [h^{-1}]	TON ^[a]	Selectivity ^[b]
1	Ph \equiv Me	1800	1100	93 (89)
2	Ph \equiv Ph Yne-2	5100	3100	81 (56)
3	Hex \equiv H Yne-3	1200 ^[c]	2200	94 ^[c] (n.d.) ^[d]
4	Pr \equiv Pr Yne-4	13200	3300	94 (92)
5	Et \equiv CH_3 Yne-5	4500	2100	93 (87)

[a] mol product/mol catalyst. [b] Measured at 50% alkyne consumption, number in parentheses measured at 99% alkyne consumption. [c] Terminal alkene selectivity. [d] C_{16} byproducts observed at high alkyne (>70%) conversion. n.d.=not determined.

uct is often a critical problem. Finally, the formation of the overhydrogenated byproduct (Ane-1) occurs only at high alkyne conversion (>90%) and at >99% consumption of Yne-1 the *Z*-selectivity decays only slightly to 89%.

We should note that Mat-Pd is much more active and selective than similar homogeneous complexes. For example, related discrete NHC–Pd⁰ complexes have a TOF of about 45 h^{-1} with a selectivity of 75% for the *Z*-alkene at 99% conversion.^[9a] Under similar conditions, the homogeneous analogue $[\text{BnMesNHC}] \text{Pd}(\text{C}_3\text{H}_5)\text{Cl}$ transforms Yne-1 to *Z*-Ene-1 with 90% selectivity at 50% conversion, although the selectivity drops to 84% at 95% conversion. The dominant byproduct of the $[\text{BnMesNHC}] \text{Pd}(\text{C}_3\text{H}_5)\text{Cl}$ -catalyzed semihydrogenation is Ane-1, which appears only at high alkyne consumption (see the Supporting Information for details). We also decomposed Mat-Pd in the absence of alkyne to give Pd⁰ particles (ca. 20 nm) that also catalyze the semihydrogenation of Yne-1, although with different rate (TOF = 700 h^{-1}) and selectivity (74% *Z*-Ene) profiles, suggesting that these particles are not the active catalyst in Mat-Pd (see the Supporting Information).

The scope of the Mat-Pd-catalyzed semihydrogenation of alkynes is shown in Table 1. Mat-Pd efficiently reduces diphenylacetylene (Yne-2), which is a challenging substrate for this reaction, to give *Z*-stilbene with 81% selectivity at 50% alkyne conversion, and 56% at >99% conversion (entry 2). This loss of selectivity at high alkyne conversion is common for Yne-2, because the product *Z*-ene-2 is known to be readily hydrogenated. 1-Octyne (Yne-3) was hydrogenated in the presence of 0.05 mol % Mat-Pd to give 1-octene in 93% selectivity at 50% conversion (entry 3). Although the semihydrogenation of 1-octyne is 86% selective for 1-octene in the C_8 fraction at 97% alkyne conversion, the formation of C_{16} byproducts at high alkyne conversion (>70%) reduces the yield of 1-octene. 4-Octyne (Yne-4) and hex-3-yne-1-ol (Yne-5) were clearly semihydrogenated to give their respective *Z*-ene products with high selectivity and activity (entries 4 and 5).

In summary, we have described the rational design and detailed DNP SENS characterization of a mesostructured silica hybrid material that contains Pd–NHC functionalities regularly distributed within the pore channels. The SENS

NMR experiments unambiguously establish the molecular environment of the Mat-Pd fragment in this hybrid material, and multidimensional NMR analysis revealed that the organometallic complex interacts with nearby $\text{-OSi}(\text{CD}_3)_3$ surface functionalities. In view of the promising catalytic efficiency in the semihydrogenation of alkynes to selectively produce Z-alkenes with this first generation of well-defined heterogeneous catalysts, we are now developing new catalysts in hope to reach higher levels of activity and stability by engineering the ligand and the surface around the supported Pd center.

Keywords: carbenes • hybrid materials • palladium • NMR spectroscopy • semihydrogenation

- [1] a) C. Copéret, M. Chabanas, R. Petroff Saint-Arroman, J.-M. Basset, *Angew. Chem.* **2003**, *115*, 164–191; *Angew. Chem. Int. Ed.* **2003**, *42*, 156–181; b) M. Tada, Y. Iwasawa, *Coord. Chem. Rev.* **2007**, *251*, 2702–2716; c) J. M. Thomas, R. Raja, D. W. Lewis, *Angew. Chem.* **2005**, *117*, 6614–6641; *Angew. Chem. Int. Ed.* **2005**, *44*, 6456–6482; d) S. L. Wegener, T. J. Marks, P. C. Stair, *Acct. Chem. Res.* **2011**, *45*, 206–214.
- [2] F. Blanc, C. Coperet, A. Lesage, L. Emsley, *Chem. Soc. Rev.* **2008**, *37*, 518–526.
- [3] A. Lesage, M. Lelli, D. Gajan, M. A. Caporini, V. Vitzthum, P. Miéville, J. Alauzun, A. Roussey, C. Thieuleux, A. Mehdi, G. Bodenhausen, C. Coperet, L. Emsley, *J. Am. Chem. Soc.* **2010**, *132*, 15459–15461.
- [4] H. Lindlar, *Helv. Chim. Acta* **1952**, *35*, 446–450.
- [5] a) M. Crespo-Quesada, A. Yarulin, M. Jin, Y. Xia, L. Kiwi-Minsker, *J. Am. Chem. Soc.* **2011**, *133*, 12787–12794; b) T. Mitsudome, Y. Takahashi, S. Ichikawa, T. Mizugaki, K. Jitsukawa, K. Kaneda, *Angew. Chem.* **2013**, *125*, 1521–1525; *Angew. Chem. Int. Ed.* **2013**, *52*, 1481–1485; c) M. Crespo-Quesada, F. Cardenas-Lizana, A.-L. Dessimoz, L. Kiwi-Minsker, *ACS Catal.* **2012**, *2*, 1773–1786.
- [6] M. Yan, T. Jin, Y. Ishikawa, T. Minato, T. Fujita, L.-Y. Chen, M. Bao, N. Asao, M.-W. Chen, Y. Yamamoto, *J. Am. Chem. Soc.* **2012**, *134*, 17536–17542.
- [7] a) H. S. La Pierre, J. Arnold, F. D. Toste, *Angew. Chem.* **2011**, *123*, 3986–3989; *Angew. Chem. Int. Ed.* **2011**, *50*, 3900–3903; b) K. Radkowski, B. Sundararaju, A. Fürstner, *Angew. Chem.* **2013**, *125*, 373–378; *Angew. Chem. Int. Ed.* **2013**, *52*, 355–360; c) G. Wienhöfer, F. A. Westerhaus, R. V. Jagadeesh, K. Junge, H. Junge, M. Beller, *Chem. Commun.* **2012**, *48*, 4827–4829; d) T. L. Gianetti, N. C. Tomson, J. Arnold, R. G. Bergman, *J. Am. Chem. Soc.* **2011**, *133*, 14904–14907; e) R. Shen, T. Chen, Y. Zhao, R. Qiu, Y. Zhou, S. Yin, X. Wang, M. Goto, L.-B. Han, *J. Am. Chem. Soc.* **2011**, *133*, 17037–17044; f) G. Vilé, B. Bridier, J. Wichert, J. Pérez-Ramírez, *Angew. Chem.* **2012**, *124*, 8748–8751; *Angew. Chem. Int. Ed.* **2012**, *51*, 8620–8623; g) J. Broggi, V. c. Jurčík, O. Songis, A. Poater, L. Cavallo, A. M. Z. Slawin, C. S. J. Cazin, *J. Am. Chem. Soc.* **2013**, *135*, 4588–4591; h) C. Oger, L. Balas, T. Durand, J.-M. Galano, *Chem. Rev.* **2012**, *112*, 1313–1350.
- [8] R. Schlägl, K. Noack, H. Zbinden, A. Reller, *Helv. Chim. Acta* **1987**, *70*, 627–679.
- [9] a) J. W. Sprengers, J. Wassenaar, N. D. Clement, K. J. Cavell, C. J. Elsevier, *Angew. Chem.* **2005**, *117*, 2062–2065; *Angew. Chem. Int. Ed.* **2005**, *44*, 2026–2029; b) P. Hauwert, G. Maestri, J. W. Sprengers, M. Catellani, C. J. Elsevier, *Angew. Chem.* **2008**, *120*, 3267–3270; *Angew. Chem. Int. Ed.* **2008**, *47*, 3223–3226; c) P. Hauwert, R. Boerleider, S. Warsink, J. J. Weigand, C. J. Elsevier, *J. Am. Chem. Soc.* **2010**, *132*, 16900–16910; d) S. Warsink, R. M. Drost, M. Lutz, A. L. Spek, C. J. Elsevier, *Organometallics* **2010**, *29*, 3109–3116; e) A. M. Kluwer, T. S. Koblenz, T. Jonischkeit, K. Woelk, C. J. Elsevier, *J. Am. Chem. Soc.* **2005**, *127*, 15470–15480.
- [10] a) T. K. Maishal, J. Alauzun, J.-M. Basset, C. Copéret, R. J. P. Corriu, E. Jeanneau, A. Mehdi, C. Reyé, L. Veyre, C. Thieuleux, *Angew. Chem.* **2008**, *120*, 8782–8784; *Angew. Chem. Int. Ed.* **2008**, *47*, 8654–8656; b) I. Karamé, M. Boualleg, J.-M. Camus, T. K. Maishal, J. Alauzun, J.-M. Basset, C. Copéret, R. J. P. Corriu, E. Jeanneau, A. Mehdi, C. Reyé, L. Veyre, C. Thieuleux, *Chem. Eur. J.* **2009**, *15*, 11820–11823; c) M. Baffert, T. K. Maishal, L. Mathey, C. Copéret, C. Thieuleux, *ChemSusChem* **2011**, *4*, 1762–1765.
- [11] F. Hoffmann, M. Cornelius, J. Morell, M. Froba, *Angew. Chem.* **2006**, *118*, 3290–3328; *Angew. Chem. Int. Ed.* **2006**, *45*, 3216–3251.
- [12] a) Ü. Akbey, W. T. Franks, A. Linden, S. Lange, R. G. Griffin, B.-J. van Rossum, H. Oschkinat, *Angew. Chem.* **2010**, *122*, 7971–7974; *Angew. Chem. Int. Ed.* **2010**, *49*, 7803–7806; b) A. Zagdoun, A. J. Rossini, M. P. Conley, W. R. Grüning, M. Schwarzwälder, M. Lelli, W. T. Franks, H. Oschkinat, C. Copéret, L. Emsley, A. Lesage, *Angew. Chem.* **2013**, *125*, 1260–1263; *Angew. Chem. Int. Ed.* **2013**, *52*, 1222–1225.
- [13] a) L. R. Becerra, G. J. Gerfen, R. J. Temkin, D. J. Singel, R. G. Griffin, *Phys. Rev. Lett.* **1993**, *71*, 3561–3564; b) M. Rosay, L. Tometich, S. Pawsey, R. Bader, R. Schauwecker, M. Blank, P. M. Borchard, S. R. Cauffman, K. L. Felch, R. T. Weber, R. J. Temkin, R. G. Griffin, W. E. Maas, *Phys. Chem. Chem. Phys.* **2010**, *12*, 5850–5860; c) D. A. Hall, D. C. Maus, G. J. Gerfen, S. J. Inati, L. R. Becerra, F. W. Dahlquist, R. G. Griffin, *Science* **1997**, *276*, 930–932; d) M. Lelli, D. Gajan, A. Lesage, M. A. Caporini, V. Vitzthum, P. Miéville, F. Héroguel, F. Rascon, A. Roussey, C. Thieuleux, M. Boualleg, L. Veyre, G. Bodenhausen, C. Copéret, L. Emsley, *J. Am. Chem. Soc.* **2011**, *133*, 2104–2107.
- [14] a) A. Zagdoun, A. J. Rossini, D. Gajan, A. Bourdolle, O. Ouari, M. Rosay, W. E. Maas, P. Tordo, M. Lelli, L. Emsley, A. Lesage, C. Copéret, *Chem. Commun.* **2012**, *48*, 654–656; b) A. Zagdoun, G. Casano, O. Ouari, G. Lapadula, A. J. Rossini, M. Lelli, M. Baffert, D. Gajan, L. Veyre, W. E. Maas, M. Rosay, R. T. Weber, C. Thieuleux, C. Copéret, A. Lesage, P. Tordo, L. Emsley, *J. Am. Chem. Soc.* **2011**, *133*, 2284–2291.
- [15] M. K. Samantaray, J. Alauzun, D. Gajan, S. Kavita, A. Mehdi, L. Veyre, M. Lelli, A. Lesage, L. Emsley, C. Copéret, C. Thieuleux, *J. Am. Chem. Soc.* **2013**, *135*, 3193–3199.

Received: June 27, 2013

Published online: August 19, 2013